Available online at www.sciencedirect.com
ScienceDirect
Journal of Power Sources 164 (2007) 849–856
JOURNAL OF POWER SOURCES
www.elsevier.com/locate/jpowsour

Kinetic characteristics of mixed conductive electrodes for lithium ion batteries

Jianxin Ma, Chunsheng Wang *, Shannon Wroblewski

Department of Chemical Engineering and Center for Manufacturing Research, Tennessee Technological University, Cookeville, TN 38505, United States

Received 23 October 2006; received in revised form 19 November 2006; accepted 20 November 2006
Available online 21 December 2006

Abstract

The rate performances of four mixed conductive electrodes ($Li_{4/3}Ti_{5/3}O_4$, $LiFePO_4$, $LiCoO_2$ and $LiCo_{1/3}Ni_{1/3}Mn_{1/3}O_2$) were investigated using galvanostatic charge/discharge, electrochemical impedance Spectroscopy (EIS) and galvanostatic intermittent titration (GITT). These four electrode materials can be roughly divided into two groups according to the structure change during Li intercalation/extraction, i.e. the phase transition materials ($Li_{4/3}Ti_{5/3}O_4$ and $LiFePO_4$) and mixed phase transformation and solid solution materials ($LiNi_{1/3}Mn_{1/3}Co_{1/3}O_2$ and $LiCoO_2$). Both the ionic conductivity and phase transition kinetics have a strong impact on the rate capability of the electrode material in addition to the generally accepted factors such as particle size and electronic conductivity. The rate capabilities of $Li_{4/3}Ti_{5/3}O_4$ and $LiFePO_4$, which have an extended flat region in the charge/discharge curves, mainly depended on their phase transition kinetics. The rate performance of the solid solution materials were controlled by the ionic conductivity, with some influence from the electronic conductivity.

Keywords: Kinetics; Cathode materials; Phase transformation; Ionic conductivity; Electronic conductivity

1. Introduction

Rechargeable lithium ion batteries have been successfully used for many portable electric devices such as cell phone and laptop computers as a power source for more than 10 years. In recent years, much effort has been focused on the development of advanced rechargeable lithium ion battery technology for use in electric powered vehicles (EVs) and/or hybrid electric vehicles (HEVs) to improve energy utilization as well as reducing environmental pollution. One of the key challenges of the current lithium ion battery technology to power the EV/HEV is its poor rate performance, which cannot meet the peak power demands for vehicular applications such as starting, accelerating, and uphill driving. The development of electrode materials with high rate capabilities, which will contribute mainly to the superior electrochemical kinetic characteristic of lithium ion batteries, is a critical issue to realize the commercialization of rechargeable lithium ion batteries as a power source for EV/HEV.

Up to now, it has been difficult to clearly depict the kinetics of the mixed conductive electrode materials used for lithium ion batteries, even though lots of efforts related to this field have been carried out [1–5]. Several factors including particle size, electronic/ionic conductivity, and phase transition kinetics (for those electrode materials, where the phase transition occurs during the charge/discharge process) have been proposed to affect the rate performance of the mixed conductive electrode material. It is well known that the rate capability of the pure $LiFePO_4$ with an electronic conductivity of $\sigma_e = 10^{-9}$ S cm^{-1} can be improved by increasing its electronic conductivity through metal doping [5] and mixing with the electronically conductive materials like carbon [6], metal [7,8] and metal oxide [9]. However, a recent result showed that the rate performance of $LiFe_{0.9}Ni_{0.1}PO_4$ with a low electronic conductivity (1.0×10^{-7} S cm^{-1}) is much better than that of $LiFePO_4$/C with a high electronic conductivity (4.0×10^{-4} S cm^{-1}) [11]. This result indicates that Li^+ diffusion capability may become a controlling step when the electronic conductivity of the $LiFePO_4$ is high. It has also been proven that the rate capability of the electrode increases with the decrease of particle size due to the short length of electronic/ionic transportations and the large specific electrochemical reaction surface [4].

* Corresponding author.
E-mail address: cswang@tntech.edu (C. Wang).

0378-7753/$ – see front matter © 2006 Elsevier B.V. All rights reserved.
doi:10.1016/j.jpowsour.2006.11.024

For example, the rate capability of $LiFePO_4$ can be markedly enhanced by decreasing its particle size [4,10]. Therefore, a balanced electronic and ionic conductivity is needed for mixed conductive electrode materials because Li^+ diffusion can occur only when accompanying electron motion is also possible. In addition, for the electrode materials in which phase transformation occurs during the charge/discharge process, it is found that the rate capability of the material may be controlled by its phase transformation kinetics if the Li diffusion and electronic conductivity are high enough. For example, a $\beta \rightarrow \alpha$ phase transformation process has been identified as a rate controlling step for the charge/discharge (hydrogen intercalation/extraction) process of $LaNi_{4.7}Al_{0.3}$ anode [12], which is similar to the Li-ion intercalation/extraction electrodes.

Therefore, it is important to distinguish these extrinsic/intrinsic effects on the electrochemical kinetics of cathode material for developing a high power electrode material. To our best knowledge, there are still no literatures discussing this issue. In the paper, we presented some preliminary results on the understanding of the electrochemical kinetics of cathode material used for lithium ion batteries. Four typical electrode materials, which can be roughly divided into two groups, i.e. the phase transition materials ($Li_{4/3}Ti_{5/3}O_4$ and $LiFePO_4$) and phase transformation-solid solution materials ($LiNi_{1/3}Mn_{1/3}Co_{1/3}O_2$ and $LiCoO_2$), were chosen in order to investigate the effect of electronic conductivity, Li-ion diffusion capability, and phase transition kinetics (for the phase transition materials) on their rate performances.

2. Experimental

2.1. Material characterizations

$LiCoO_2$ and $Li_{4/3}Ti_{5/3}O_4$ powders were received from Altair Technologies, $LiFePO_4$ powder from Phostech Lithium Inc., and $LiNi_{1/3}Mn_{1/3}Co_{1/3}O_2$ powder from the University of Texas at Austin. The micro-morphology of the electrode materials was observed by scanning electron microscopy (SEM) images using a FEI Quanta 200 with Electron Diffraction Spectrometer (EDS). The electronic/ionic conductivity of the materials was evaluated with electrochemical impedance spectroscopy (EIS) using blocking electrodes. The blocking disc electrodes were prepared by die-pressing powders (without any additive) with a pressure of 3 tonnes cm^{-2}, and then coating with Ag paste on both sides of the discs followed by drying under atmosphere. The sizes of the discs were 1.27 cm in diameter with a thickness of about 0.1 cm. The electronic/ionic conductivity of the disc was measured by EIS using the Solartron 1260/1287 method with the frequency range of 32 MHz to 1 Hz at the potentiostatic sine wave signal amplitude of 50 mV, and was then calculated using the equivalent circuit proposed by Jamnik and Maier [13,14].

2.2. Electrode and cell preparation

The electrodes used for electrochemical performance measurement were prepared using following procedures. The mixture of active material, carbon black and polyvinylidene fluoride (PVDF, Kynar™, Elf-Atochem) in 1-methyl-2-pyrrolidinone solvent with a weight ratio of 80:10:10 was formed into a viscous paste. The resulting viscous paste was homogenized in an ultrasonic bath for 30 min and stirred thoroughly before use. The obtained paste was then coated uniformly on a sheet of carbon-coated Al foil (carbon-coated Cu foil for $Li_{4/3}Ti_{5/3}O_4$) using a doctor blade. The film was then dried in vacuum oven at 120 °C overnight. After cooling down to room temperature, the sheet was punched into a disc with the diameter of 1.27 cm and was used as a testing electrode. The loading of active material was about 5.0 mg cm^{-2}.

Electrochemical performance of the electrode material was carried out using a coin cell (size 2025). All testing cells were assembled in an argon-filled glove box, which consisted of the cathode (working electrode), lithium foil as the anode, a composition of 1.0 M $LiPF_6$ in EC-DEC-DMC-EMC (1:1:1:3 by volume) (Ferro Corporation) as the liquid electrolyte, and a polypropylene (PP) microporous film as the separator. Before testing the electrochemical performance, the cells were activated through several charge/discharge cycles with a small current ($0.1C$, $1C = 150$ mA g^{-1} for all the materials studied) using an Arbin Corporation (College Station, TX) automatic battery cycler.

2.3. Electrochemical performances measurement

For the discharge (Li intercalation) rate performance measurements, the cells were charged at $0.1C$ rate current to the upper cut-off voltage, and then discharged at the different rate currents to the lower cut-off voltage. Due to the difference in the equilibrium potentials of the four electrodes, the cut-off voltage windows for $Li_{4/3}Ti_{5/3}O_4$, $LiFePO_4$, $LiCoO_2$ and $LiNi_{1/3}Mn_{1/3}Co_{1/3}O_2$ were designed to 0.8–2.5, 2.0–4.2, 2.7–4.3 and 2.7–4.3 V, respectively. The rate capabilities of the electrode materials at the different discharge currents were evaluated using the ratio of the capacity at a given current to the capacity at $0.1C$.

The thermodynamic properties of the electrode materials such as maximum capacity, equilibrium potential, and potential hysteresis between the charge and discharge were obtained using the galvanostatic intermittent titration (GITT) technique at a low current density of $0.02C$. The electrodes were charged and discharged by the use of a series of intermittent current for 1.0 h, leaving the electrode at open circuit for 2.0 h between each intermittent current, and the cell voltages after the rest time of 2.0 h were recorded as the open circuit voltage (OCV) of the half cell at a given state of discharge.

3. Results and discussion

3.1. Charge/discharge behavior at a low cycling current

The charge/discharge behaviors of the materials at a $0.1C$ current density are shown in Fig. 1. For $Li_{4/3}Ti_{5/3}O_4$ electrode (Fig. 1a), the charge/discharge curve is characterized by a very flat and extended voltage plateau at around 1.55 V, which is a typical characteristic of phase transition between a Li-

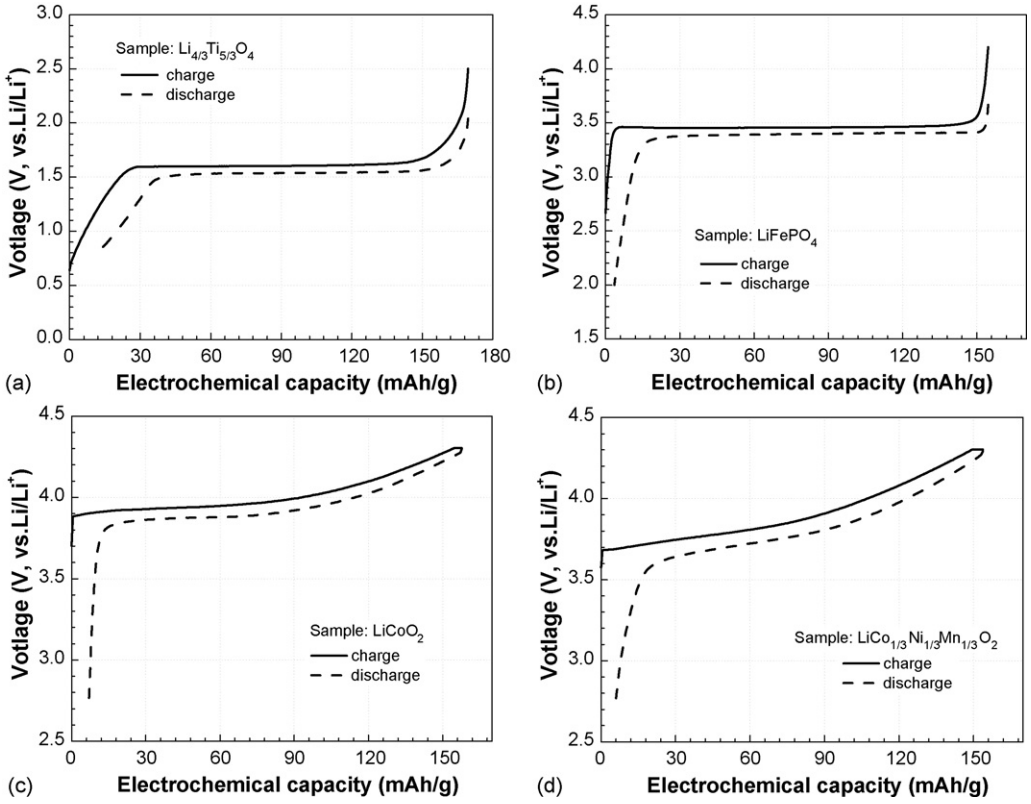

Fig. 1. Voltage profiles of (a) $Li_{4/3}Ti_{5/3}O_4$, (b) $LiFePO_4$, (c) $LiCoO_2$ and (d) $LiCo_{1/3}Ni_{1/3}Mn_{1/3}O_2$ at an charge/discharge current of 15 mA g^{-1}.

rich phase (rocksalt, $Li_{7/3}Ti_{5/3}O_4$) and a Li-poor phase (spinel, $Li_{4/3}Ti_{5/3}O_4$) as proposed by Ohzuku et al. [15].

$$(\mathrm{Li})8a(\mathrm{Li}_{1/3}, \mathrm{Ti}_{4/3})16dO_4 + e^- + Li^+ = (\mathrm{Li}_2)16c(\mathrm{Li}_{1/3}, \mathrm{Ti}_{4/3})16dO_4$$

The experimentally determined specific discharge capacity of $Li_{4/3}Ti_{5/3}O_4$ is 157.6 mAh g, which is 94.1% of the theoretical value (167.5 mAh g^{-1}).

Similar to the $Li_{4/3}Ti_{5/3}O_4$ electrode, the electrochemical charge/discharge profile of $LiFePO_4$ sample (Fig. 1b) also shows a flat domain over a large compositional range at around 3.4 V, which was attributed to the two-phase reaction between $LiFePO_4$ and $FePO_4$ phase.

$$Li^+ + e + FePO_4\,(\text{heterosite phase}) = LiFePO_4(\text{triphylite phase})$$

The electrochemical reversible capacity of the sample was 151.1 mAh g^{-1}, which was 88.9% of the theoretical value (170 mAh g^{-1}).

Different from the samples mentioned above, the charge/discharge behaviors of the $LiCoO_2$ sample (Fig. 1c) presented a combination of a sloping line and a flat domain in the voltage profile. During the discharge (Li intercalation) process, the voltage of Li_xCoO_2 decreased gradually with the increase of Li content first (correspondent to $100 < Q < 157$ mAh g^{-1}), and then kept an almost constant value in the capacity range $10 < Q < 90$ mAh g^{-1}. The charge/discharge voltage profile of $LiCoO_2$ indicated that inserted lithium first formed a solid solution and then phase transformation occurred when Li content is over the solubility limit. Therefore, the charge/discharge of $Li_{1-x}CoO_2$ was combined with solid solution domains and a two-phase transformation, which is in agreement with the previous results [16,17].

The charge/discharge profile of $LiNi_{1/3}Mn_{1/3}Co_{1/3}O_2$ (Fig. 1d) was slightly different from $LiCoO_2$, showing a rapid voltage change with Li content in the high Li content range and a slow voltage variation (or a sloppy voltage plateau) in the low Li content area. Therefore, partial replacement of Co with Ni and Mn in $LiCoO_2$ changed the phase transformation process, resulting in a sloppy potential plateau. The charge/discharge characteristic of the material presented here was similar to that observed by others [18–20]. However, the electrochemical capacity of the material was 148.2 mAh g^{-1} when the voltage was changed between 2.7 and 4.3 V, which was lower than the result (about 200 mAh g^{-1}) reported in the literatures [19,20] due to the wide potential window (2.7–4.6 V) used in their work.

Based on the charge/discharge behaviors at a low current, these four electrode materials under investigation can be roughly divided into two groups according to the charge–discharge profiles, i.e. the phase transformation materials ($Li_{4/3}Ti_{5/3}O_4$ and $LiFePO_4$) and phase transformation-solid solution materials ($LiNi_{1/3}Mn_{1/3}Co_{1/3}O_2$ and $LiCoO_2$). The discharge rate capability of these materials and the effects of extrinsic/intrinsic factors on their rate performances will be addressed at the following sections.

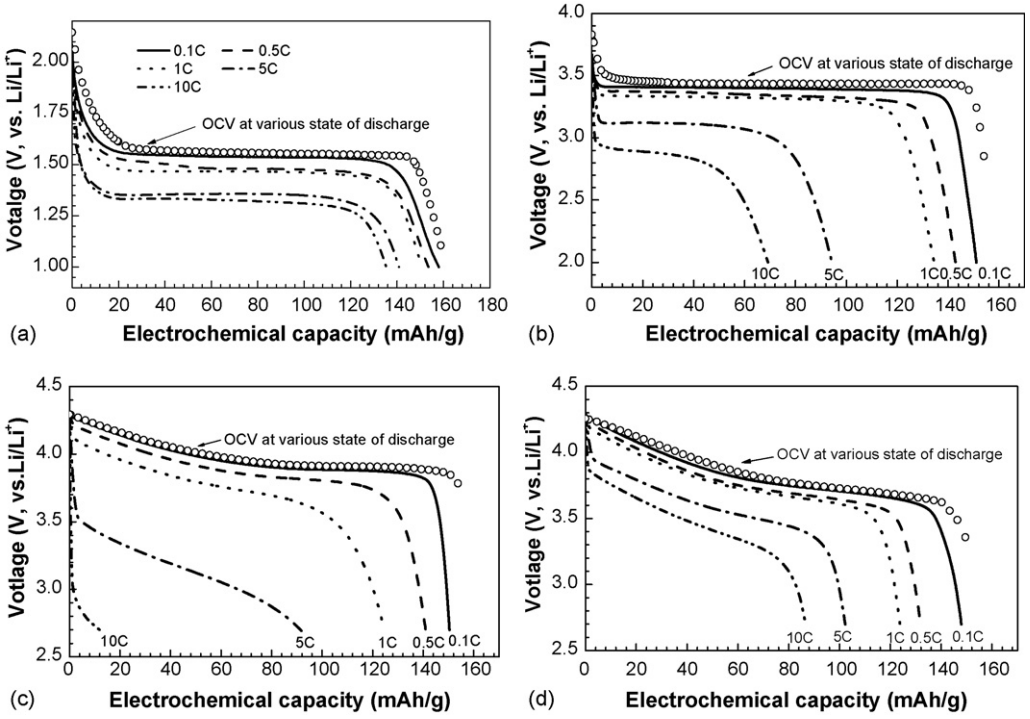

Fig. 2. Voltage profiles of (a) $Li_{4/3}Ti_{5/3}O_4$, (b) $LiFePO_4$, (c) $LiCoO_2$, and (d) $LiCo_{1/3}Ni_{1/3}Mn_{1/3}O_2$ at different discharge *C* rate after charging to the upper cut-off potential at 15 mA g^{-1}. The open circuit voltages (open dot) at different state of discharge measured using GITT are also shown for comparison.

3.2. Rate performance

The discharge behaviors of the four materials measured at the different *C* rate currents are shown in Fig. 2. The open circuit voltages at different state of discharge measured using GITT are also shown in Fig. 2 for comparison. The discharge capacities (utilizations of the active materials) and the overvoltages (voltage drop) of the electrode increased with the discharge current. The overvoltages of the electrodes at the same discharge current increased in order of $Li_{4/3}Ti_{5/3}O_4 < LiCo_{1/3}Ni_{1/3}Mn_{1/3}O_2 < LeFePO_4 < LiCoO_2$. Carefully comparing the discharge profiles of $Li_{4/3}Ti_{5/3}O_4$ with that of $LiFePO_4$, one can find that the decrease in capacity and the increase in overvoltage of $Li_{4/3}Ti_{5/3}O_4$ in the voltage plateau (phase transformation) region were less than that of $LiFePO_4$ at the same discharge current. For $LiCoO_2$ and $LiCo_{1/3}Ni_{1/3}Mn_{1/3}O_2$ electrodes, which consist of the solid solution and phase transformation during discharge process, the discharge capacity in the two-phase region was more sensitive to the discharge current than that in the solid solution region. This result suggested that kinetics of phase transformation in two-phase region played a very important role in the rate capability of the electrodes. The higher rate capability of $LiCo_{1/3}Ni_{1/3}Mn_{1/3}O_2$ compared to $LiCoO_2$ is in agreement with the reported results [20] and is probably due to the sloppy potential plateau of $LiCo_{1/3}Ni_{1/3}Mn_{1/3}O_2$ in the two-phase region which looks like a solid solution.

Assuming the discharge capacity of the materials under 0.1*C* is 100%, the normalized rate capabilities of $Li_{4/3}Ti_{5/3}O_4$, $LiFePO_4$, $LiCoO_2$ and $LiCo_{1/3}Ni_{1/3}Mn_{1/3}O_2$ under 10*C* are 82, 50, 10 and 60% of their capacities at 0.1*C*, respectively. Fig. 3 shows the rate capability of the $Li_{4/3}Ti_{5/3}O_4$, $LiFePO_4$, $LiCoO_2$ and $LiCo_{1/3}Ni_{1/3}Mn_{1/3}O_2$ at different *C* rates. The rate capabilities of the four electrodes increased in order of $LiCoO_2 < LiFePO_4 < LiCo_{1/3}Ni_{1/3}Mn_{1/3}O_2 < Li_{4/3}Ti_{5/3}O$. Since the loading of active material, and the amount of carbon and PVDF additions are the same in the four composite electrodes, the rate capabilities of the composite electrodes should reflect the intrinsic characteristics of the electrode materials. The excellent rate capability of $Li_{4/3}Ti_{5/3}O_4$ was in agreement with the results reported by others [21–23]. For example, Kavan et al. reported that nanocrystalline $Li_{4/3}Ti_{5/3}O_4$ exhibited excellent activity toward Li intercalation even at charging rates as high as 250*C* [21]. Pure $LiFePO_4$ has been proven to have a poor electrochemical kinetic characteristic due

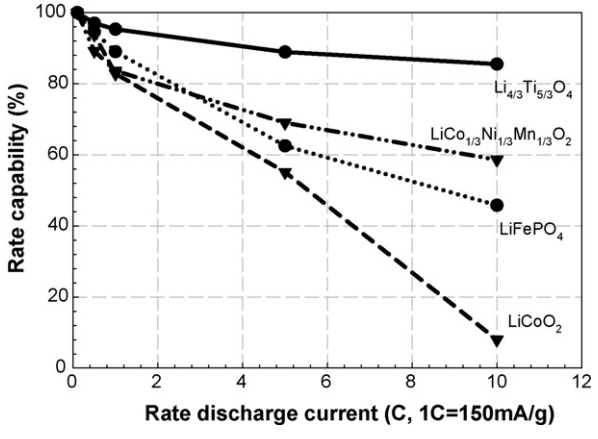

Fig. 3. Discharge rate capability of these four electrode materials under studied.

Table 1
Electronic/ionic conductivities and discharge capacity of the four electrode materials

Sample	σ_e (S cm^{-1})	σ_i (S cm^{-1})	Capacity at 0.1C (mAh g^{-1})	Capacity at 10C (mAh g^{-1})
$Li_{4/3}T_{5/3}O$	3.9×10^{-8}	2.5×10^{-5}	158.1	135.4
$LiFePO_4$	5.0×10^{-4}	1.5×10^{-5}	151.1	69.2
$LiCoO_2$	7.7×10^{-7}	5.5×10^{-4}	150.4	11.9
$LiCo_{1/3}Ni_{1/3}Mn_{1/3}O_2$	2.5×10^{-7}	1.3×10^{-3}	147.9	86.6

to its low electronic conductivity ($\sim 10^{-9}$ S cm^{-2}) [5]. $LiFePO_4$ presented here showed a better rate capability than that of $LiCoO_2$ because the material developed by Phostech Lithium Inc. was coated with carbon on the surface of the particles [24].

In the following several sections, the effect of electronic conductivity, Li diffusion coefficient (or ionic conductivity), particle size and phase transition on the rate capability of the electrode materials is discussed based on the experimental results.

3.3. Electronic conductivity of the electrode materials

It is well known that the rate performance of $LiFePO_4$ and $Li_{4/3}Ti_{5/3}O_4$ electrodes can be greatly improved by enhancing their electronic conductivity [5,7–10,25]. Also, all four electrode materials are mixed electronic/ionic conductors. One immediate hypothesis is that the increase in the rate performance for the four materials ($LiCoO_2 < LiFePO_4 < LiCo_{1/3}Ni_{1/3}Mn_{1/3}O_2 < Li_{4/3}Ti_{5/3}O$) is probably determined by their electronic conductivities. Table 1 listed the electronic conductivities of the four electrode materials measured using the impedance technique. The electronic conductivities of the four materials increase in order of $Li_{4/3}Ti_{5/3}O_4 < LiCo_{1/3}Ni_{1/3}Mn_{1/3}O_2 < LiCoO_2 < LiFePO_4$. The trend of the increase in the electronic conductivity is almost in reverse order of the rate capability (Fig. 3). As a white powder, the electronic conductivity of $Li_{4/3}Ti_{5/3}O_4$ showed the lowest electronic conductivity (10^{-8} S cm^{-1}), although its rate capability was the best in the four materials. The conductivity of 10^{-8} S cm^{-1} for $Li_{4/3}Ti_{5/3}O_4$ was in agreement with the data reported in the literature [26]. One possible argument for the high rate capability of $Li_{4/3}Ti_{5/3}O_4$ is that the low-electron-conductive $Li_{4/3}Ti_{5/3}O_4$ is covered by a high-electron-conductive (10^{-2} S cm^{-1} [27]) layer (Li-rich phase, $Li_{7/3}Ti_{5/3}O_4$) during the discharge (lithium intercalation) process (Fig. 4). The highly conductive outer-layer formed a continuous conductive web in the electrode which greatly enhanced the Li intercalation rate capability of $Li_{4/3}Ti_{5/3}O_4$. If this is the case, the low-electron-conductor, $Li_{4/3}Ti_{5/3}O_4$, will be covered on the surface by $Li_{7/3}Ti_{5/3}O_4$ during Li extraction, therefore, the rate capability of $Li_{7/3}Ti_{5/3}O_4$ in Li extraction should be much worse than that in Li intercalation. Fig. 5 shows the charge (Li extraction) behavior of $Li_{7/3}Ti_{5/3}O_4$ at different charge C rate currents. The charge rate performance (Fig. 5) is almost the same with the discharge rate performance (Fig. 2a) at the same C rate current, which indicates that the superior discharge rate performance of $Li_{4/3}Ti_{5/3}O_4$ is not due to formation of a high-electron-conductive $Li_{7/3}Ti_{5/3}O_4$ out-layer. In addition, among these four materials, the electronic conductivity of $LiFePO_4$ ($\sim 10^{-4}$ S cm^{-1}) is four orders of magnitude higher than that of $Li_{4/3}Ti_{5/3}O_4$. But, the rate capability of $LiFePO_4$ is inferior to $Li_{4/3}Ti_{5/3}O_4$, which inferred that the rate capabilities of the different cathode materials were not controlled by their electronic conductivities. However, for the individual material such as pure $LiFePO_4$ with a much lower intrinsic electronic conductivity (10^{-9} S cm^{-1}), the rate capability can be enhanced by increasing its electronic conductivity initially. When the electronic conductivity of the material is over a threshold value, however, its rate capability will not be determined by the electronic conductivity but by some other factors such as the Li diffusion coefficient, particle size, and phase transition kinetic.

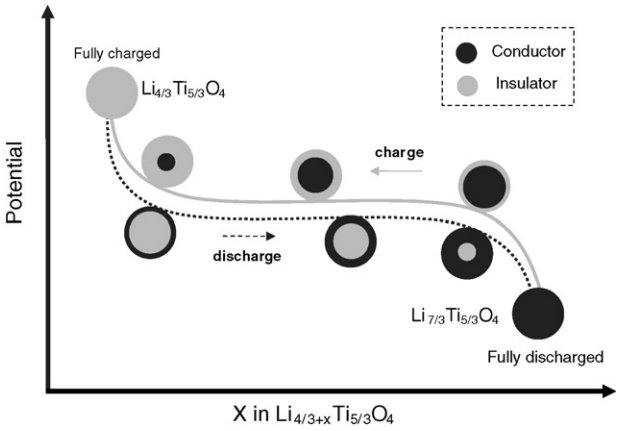

Fig. 4. Illustration of the charge/discharge process of $Li_{4/3}Ti_{5/3}O_4$.

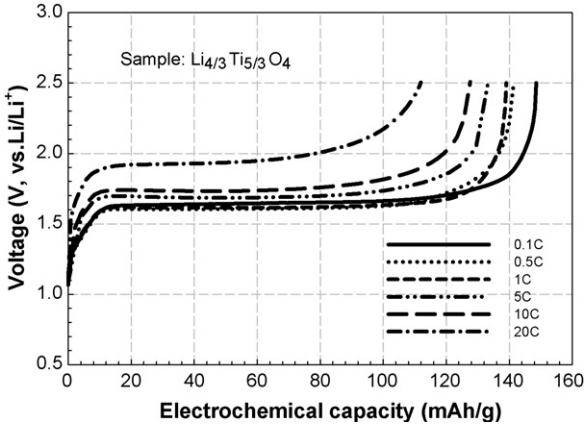

Fig. 5. Voltage profiles of $Li_{4/3}Ti_{5/3}O_4$ during charge at different current densities after fully discharged.

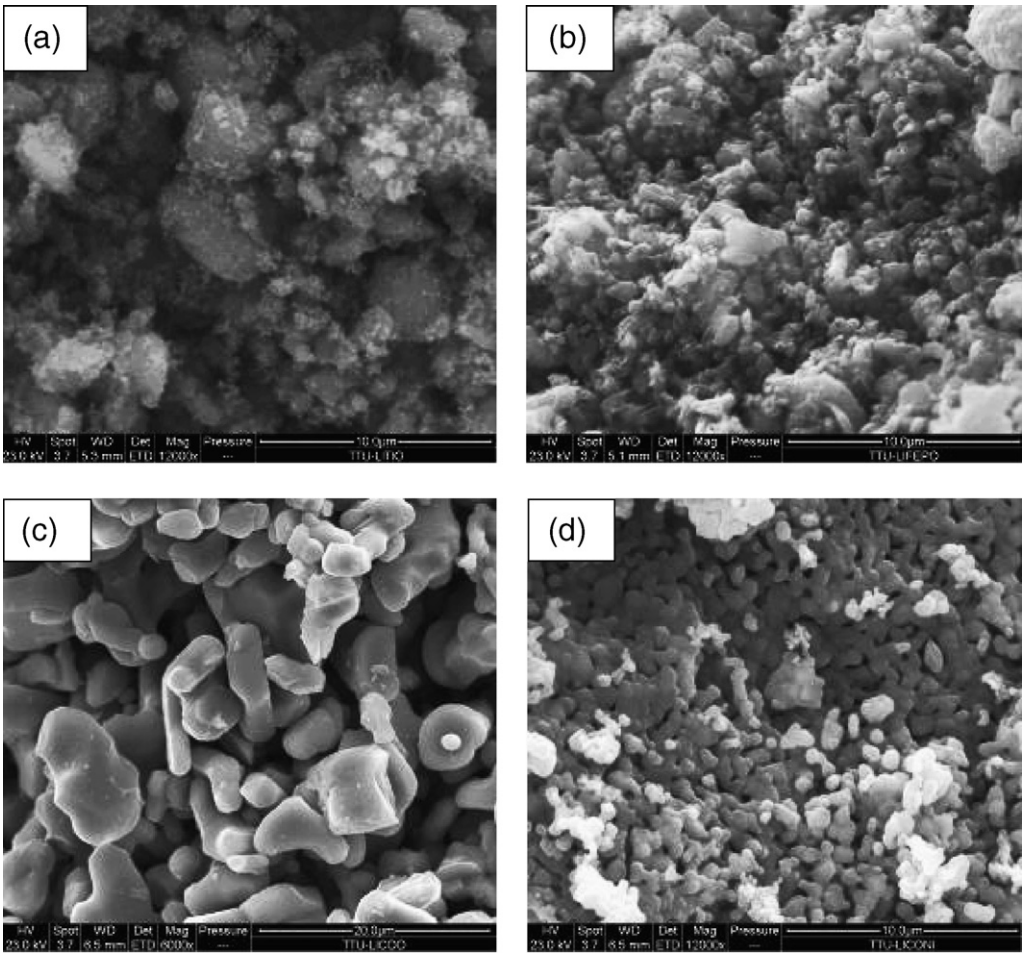

Fig. 6. SEM images of the materials, (a) $Li_{4/3}Ti_{5/3}O_4$, (b) $LiFePO_4$, (c) $LiCoO_2$, and (d) $LiCo_{1/3}Ni_{1/3}Mn_{1/3}O_2$, the magnifications in (a, b and d) are 12K×, and the magnification in (c) is 6K×.

3.4. Li-ion diffusion capability and particle size of the materials

Li-ion diffusion capability in the electrode materials depends both on extrinsic parameter and intrinsic parameter of the material, the former includes particle size and the distribution of particle size (DPS), while the latter includes diffusion coefficient of lithium ion within the material. For an electrode material with a fixed Li-ion diffusion coefficient, the Li-ion diffusion capability of the material decreases with the increase of particle size due to the long Li diffusion path in a particle. For various electrode materials with the same particle size, Li-ion diffusion capability will be controlled by the Li-ion diffusion coefficient. For comparison of Li-ion diffusion

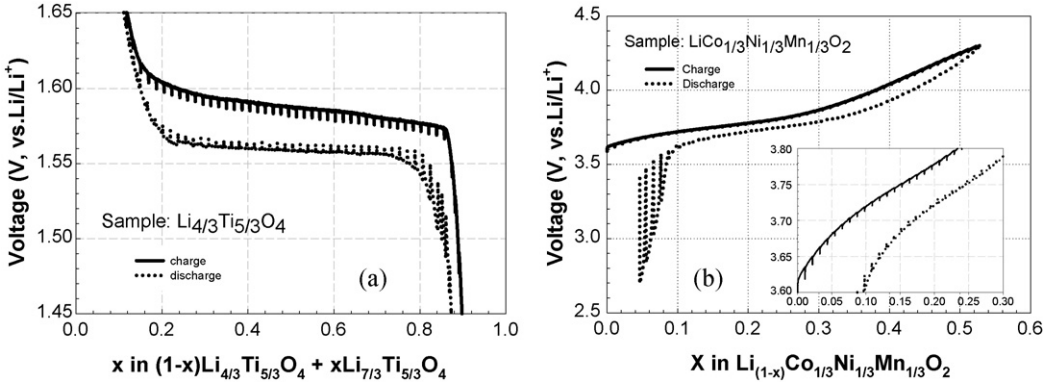

Fig. 7. Galvanostatic intermittent charge and discharge curves of (a) $Li_{4/3}Ti_{5/3}O_4$ and (b) $LiCo_{1/3}Ni_{1/3}Mn_{1/3}O_2$ measured using the GITT technique at a current of 3 mA g^{-1} at 25 °C. The electrode was charged and discharged by the use of series of intermittent current for 1.0 h, leaving the electrode at open circuit for 2.0 h between each intermittent current.

Table 2
Rate performance and its effecting factors

Rate capability and its effecting factors	Order of the electrode material
Rate capability	$Li_{4/3}Ti_{5/3}O_4 > LiCo_{1/3}Ni_{1/3}Mn_{1/3}O_2 > LiFePO_4 > LiCoO_2$
Electronic conductivity	$LiFePO_4 > LiCoO_2 > LiCo_{1/3}Ni_{1/3}Mn_{1/3}O_2 > Li_{4/3}Ti_{5/3}O_4$
Li-ion diffusion capability	$LiCo_{1/3}Ni_{1/3}Mn_{1/3}O_2 > Li_{4/3}Ti_{5/3}O_4 > LiFePO_4 > LiCoO_2$
Phase transition kinetics	$Li_{4/3}Ti_{5/3}O_4 > LiCo_{1/3}Ni_{1/3}Mn_{1/3}O_2$
Combination of phase transformation and Li-ion diffusion capability	$Li_{4/3}Ti_{5/3}O_4 > LiCo_{1/3}Ni_{1/3}Mn_{1/3}O_2 > LiFePO_4 > LiCoO_2$

capability of electrode material, therefore, both extrinsic characteristics (such as particle size and size distribution) and intrinsic characteristics (diffusion coefficient) of the material should be considered comprehensively. Since the diffusion capability of the material is in inverse proportion to square of particle size and in proportion to diffusion coefficient (D/r^2), the particle size has stronger impact on the diffusion capability than the diffusion coefficient. Therefore, the particle sizes of these four electrode materials were estimated using SEM images as shown in Fig. 6. Carefully compared to the SEM image of these materials, some differences in the particle size and morphology characteristics of the materials can be distinguished. Among all the materials, the particle size of $LiCoO_2$ is the largest (5–10 μm), which has almost one order magnitude higher than that of the other samples. Therefore, the poor kinetic characteristic of $LiCoO_2$ can be mainly attributed to its large particle size. Since the particle sizes of $Li_{4/3}Ti_{5/3}O_4$, $LiFePO_4$ and $LiCo_{1/3}Ni_{1/3}Mn_{1/3}O_2$ are similar but their rate capabilities are quite different (Fig. 3), the ionic conductivity of the four electrode materials were measured using EIS, and also listed in Table 1. The reasons for measuring the ionic conductivity of the electrode materials rather than their diffusion coefficients of four electrodes are: (1) the accurate Li-ion diffusion coefficient of phase transition material cannot be obtained by the standard EIS and GITT methods in a three-electrode-cell due to the phase transition (rather than composition variation) during measurement; (2) an accurate ionic conductivity of phase transition electrode can be measured using EIS and blocking electrode and the diffusion coefficient of Li-ions can be calculated from the ionic conductivity using the Nernst–Einstein equation. It can be found that the ionic conductivity of the materials increased in the order of $LiFePO_4 < Li_{4/3}Ti_{5/3}O_4 < LiCoO_2 < LiCo_{1/3}Ni_{1/3}Mn_{1/3}O_2$. Although Li-ion diffusion coefficient of $LiCoO_2$ is high up to $\sim 10^{-4}\,S\,cm^{-1}$, $LiCoO_2$ still has the lowest Li-ion diffusion capability due to its large particle size because the particle size has stronger impact on the diffusion capability than the diffusion coefficient (diffusion capability = D/r^2). Considering the particle size and ionic conductivity, Li^+ ion diffusion capability of the four materials can be rearranged with following orders: $LiCoO_2 < LiFePO_4 < Li_{4/3}Ti_{5/3}O_4 < LiCo_{1/3}Ni_{1/3}Mn_{1/3}O_2$.
When compared with the rate capability order of the four materials, the $Li_{4/3}Ti_{5/3}O_4$ and $LiCo_{1/3}Ni_{1/3}Mn_{1/3}O_2$ were still in a reversed position, which indicated that factors other than electronic and ionic conductivity may determine the rate performance of $Li_{4/3}Ti_{5/3}O_4$ and $LiCo_{1/3}Ni_{1/3}Mn_{1/3}O_2$.

3.5. Phase transformation

The effect of phase transition on rate capability of electrode material can be distinguished by comparing the electrochemical performance of $Li_{4/3}Ti_{5/3}O_4$ and that of $LiCo_{1/3}Ni_{1/3}Mn_{1/3}O_2$ under different discharge current. As shown in Fig. 2d, the low capacity of $LiCo_{1/3}Ni_{1/3}Mn_{1/3}O_2$ at a high discharge current was mostly attributed to the capacity lost in the phase transition region, while the capacity in the solid solution region is almost the same even at a high discharge current. Therefore, the phase transformation in $LiCo_{1/3}Ni_{1/3}Mn_{1/3}O_2$ becomes difficult when discharge current is high. However, $Li_{4/3}Ti_{5/3}O_4$ still has considerable capacity even at a high discharge current, indicating phase transformation in $Li_{4/3}Ti_{5/3}O_4$ is much easier than that of $LiCo_{1/3}Ni_{1/3}Mn_{1/3}O_2$. Therefore, the phase transformation kinetics may be the reason for the difference of rate performance between $Li_{4/3}Ti_{5/3}O_4$ and $LiCo_{1/3}Ni_{1/3}Mn_{1/3}O_2$.

The faster phase transformation of $Li_{4/3}Ti_{5/3}O_4$ than that of $LiCo_{1/3}Ni_{1/3}Mn_{1/3}O_2$ is due to zero volume change during phase transformation for $Li_{4/3}Ti_{5/3}O_4$. The phase transformation resistance also can be partly evaluated by the potential hysteresis between charge and discharge. Fig. 7 presents the galvanostatic intermittent charge and discharge curves of $Li_{4/3}Ti_{5/3}O_4$ and $LiCo_{1/3}Ni_{1/3}Mn_{1/3}O_2$. $Li_{4/3}Ti_{5/3}O_4$ shows a much narrower potential hysteresis than $LiCo_{1/3}Ni_{1/3}Mn_{1/3}O_2$ due to zero volume change of $Li_{4/3}Ti_{5/3}O_4$ during the Li intercalation/extraction process. For the case of $Li_{4/3}Ti_{5/3}O_4$, the equilibrium potential (EP) hysteresis between the charge process (lithium extraction) and the discharge process (lithium intercalation) was about 10 mV, which was higher than the value (about 4 mV) reported in the literature [27]. The reason for this can be attributed to the use of a different measuring method. In our case, the galvanostatic intermittent charge and discharge curves of the samples were measured with charge/discharge for 1 h followed by rest for 2 h, while the GITT in the literature [27] were measured by charge/discharge for 17 min followed by rest until the potential slope with time is less than $0.7\,mV\,h^{-1}$. The rest time in the literature is much longer than that used here. During the zero volume change in the phase transformation between $Li_{4/3}Ti_{5/3}O_4$ and $Li_{7/3}Ti_{5/3}O_4$, the EP hysteresis resulting from the phase transformation should be zero. The observed EP hysteresis can be attributed to the heterosphere charge/discharge properties of a porous electrode [28]. The potential hysteresis of $LiCo_{1/3}Ni_{1/3}Mn_{1/3}O_2$ was almost 50 mV, which was much higher than that of $Li_{4/3}Ti_{5/3}O_4$. It was reported that the volume change of $Li_{1-x}CoO_2$ ($x = 0$–0.5) during charge/discharge process was about 2% [29], which was much higher than

that of $Li_{4/3}Ti_{5/3}O_4$. Therefore, the large potential hysteresis of $LiCo_{1/3}Ni_{1/3}Mn_{1/3}O_2$ can be attributed to its larger volume change during the charge/discharge process.

4. Summary

In this work, four mixed electron/ion conductive electrode materials including $Li_{4/3}Ti_{5/3}O_4$, $LiFePO_4$, $LiCoO_2$ and $LiCo_{1/3}Ni_{1/3}Mn_{1/3}O_2$ were chosen to investigate the rate performance. According to the structure change during Li intercalation and extraction, these four electrode materials can be roughly divided into two groups, i.e. the phase transition materials ($Li_{4/3}Ti_{5/3}O_4$ and $LiFePO_4$) and phase transformation-solid solution materials ($LiNi_{1/3}Mn_{1/3}Co_{1/3}O_2$ and $LiCoO_2$).

The effect of electronic conductivity, Li-ion diffusion capability and phase transition kinetic (for the phase transition materials) on the rate capability of these materials is summarized in Table 2. The results indicate that the rate capability of the electrode materials is mainly controlled by phase transformation kinetics and then Li-ion diffusion capability, although the electronic conductivity of the materials also affects the rate performance. The best rate capability of $Li_{4/3}Ti_{5/3}O_4$ is due to the fast phase transformation with zero volume change, and the good rate performance of $LiCo_{1/3}Ni_{1/3}Mn_{1/3}O_2$ is attributed to the high Li-ion diffusion capability. The reasonable rate behavior of $LiFePO_4$ is attributed to the balanced phase transformation kinetics and Li-ion diffusion ability. The worst rate performance of $LiCoO_2$ is due to the large particle size. The electronic conductivity is less important than others is because 5–10 wt% carbon black is normally mixed into electrodes which enhanced the electronic conductivity. However, if the electronic conductivity of the electrode materials is too low (less than 10^{-8} S cm^{-1}), the improvement of the electronic conductivity of the materials will greatly improve the rate performance.

References

[1] G.S. Nagarajan, J.W. Van Zee, R.M. Spotnitz, J. Electrochem. Soc. 145 (1998) 771.
[2] V. Srinivasan, J. Newman, J. Electrochem. Soc. 151 (2004) A1517.
[3] R.E. Garcia, Y.M. Chiang, W.C. Carter, P. Limthongkul, C.M. Bishop, J. Electrochem. Soc. 152 (2005) A255.
[4] A. Yamada, S.C. Chung, K. Hinokuma, J. Electrochem. Soc. 148 (2001) A224.
[5] S.Y. Chung, J. Bloking, Y.M. Chiang, Nature Mat. 1 (2002) 123.
[6] H. Huang, S.C. Yin, L.F. Nazar, Electrochem. Solid State Lett. 4 (2001) A170.
[7] K.S. Park, J.T. Son, H.T. Chung, S.J. Kim, C.H. Lee, K.T. Kang, H.G. Kim, Solid State Commun. 129 (2004) 311.
[8] F. Croce, A. Depifanio, J. Hassoun, A. Deptula, T. Olczac, B. Scrosati, Electrochem. Solid State Lett. 5 (2002) A47.
[9] A. Depifanio, F. Croce, P. Reale, L. Settimi, B. Scrosati, Proceedings of the 203rd ECS Meeting, vol. 27, Paris, April 2 May, 2003 (Abstract No. 1114).
[10] J. Lu, Z. Tang, Z. Zhang, W. Shen, Mater. Res. Bull. 40 (2005) 2039.
[11] D. Wang, H. Li, S. Shi, X. Huang, L. Chen, Electrochim. Acta 50 (2005) 2955.
[12] F. Feng, J. Han, M. Geng, D.O. Northwood, Solar Energy Mater. Solar Cells 62 (2005) 51.
[13] J. Jamnik, J. Maier, J. Electrochem. Soc. 146 (1999) 4183.
[14] J. Jamnik, Solid State Ionics 157 (2003) 19.
[15] T. Ohzuku, A. Ueda, N. Yamamoto, J. Electrochem. Soc. 142 (1995) 1431.
[16] J.N. Reimers, J.R. Dahn, J. Electrochem. Soc. 139 (1992) 2091.
[17] M. Menetrier, I. Saadoune, S. Levasseur, C. Delmas, J. Mater. Chem. 9 (1999) 1135.
[18] K.M. Shaju, G.V. Subba, B.V.R. Chowdari, J. Electrochem. Soc. 151 (2004) A1324.
[19] N. Yabuuchi, T. Ohzuku, J. Power Sources 119–121 (2003) 171.
[20] K.M. Shaju, G.V.S. Rao, B.V.R. Chowdari, Electrochim. Acta 48 (2002) 145.
[21] L. Kavan, J. Prochazka, T.M. Spitler, M. Kalbac, M. Zukalova, T. Drezen, M. Gratzel, J. Electrochem. Soc. 150 (2003) A1000.
[22] K. Nakahara, R. Nakajima, T. Matsushima, H. Majuma, J. Power Sources 117 (2003) 131.
[23] J.L. Allen, T.R. Jow, J. Wolfensitne, J. Power Sources 159 (2006) 1340.
[24] D. Geoffroy, N. Ravet, 21st International Seminar & Exhibit on Primary & Secondary Batteries, Fort Lauderdale, Florida, March, 2004.
[25] J. Wolfenstine, U. Lee, J.L. Allen, J. Power Sources 154 (2006) 287.
[26] N.V. Porotnikov, N.G. Chaban, K.I. Petrov, Izv. Akad. Nauk SSSR, Neorg. Mater. 18 (1982) 1066.
[27] S. Scharner, W. Weppner, P. Schmid-Beurmann, J. Electrochem. Soc. 146 (1999) 857.
[28] B. Wu, M. Mohammed, D. Brigham, R. Eldewr, R.E. White, J. Power Sources 101 (2001) 149.
[29] J.N. Reimers, J.r. Dahn, J. Electrochem. Soc. 139 (1992) 2091.